

Paper Type: Original Article

Effect of Graft Geometric Parameters on Shear Stress Applied to the Coronary Artery in Bypass Surgery

Khadije Moradian^{1,*} , Fatemeh Dehghan¹

¹Department of Mechanical Engineering, University of Birjand, Birjand, Iran; moradiankhadije@gmail.com.

²Department of Science in Electrical Engineering, Noavaran-e Binsh, Tehran, Iran; F_Deighan@gmail.com.

Citation:

Received: 17 January 2025

Revised: 24 August 2025

Accepted: 22 October 2025

Moradian, K., & Dehghan, F. (2025). Effect of graft geometric parameters on shear stress applied to the coronary artery in Bypass Surgery. *Mechanical Technology and Engineering Insights*, 2(4), 233-239.


Abstract


Cardiovascular Diseases (CVDs) are among the most common causes of death worldwide. One of the treatment methods is grafting a vessel from the upstream area to the aortocoronary artery and from the downstream area to the region beyond the coronary artery blockage, performed during bypass surgery. In the present study, the effect of geometric parameters (graft angles and distances) on velocity and Wall Shear Stress (WSS) applied to the coronary artery is investigated. The maximum velocity occurs at the center of the stenosis in the main vessel, decreasing toward the wall. An increase in velocity gradient leads to increased shear stress, which may damage the vessel wall. The maximum velocity and minimum shear stress occur at a 5-degree angle. The optimal condition for surgery at 95% stenosis is a graft angle of 15 degrees and a distance of 10 mm from the stenosis location, because the shear stress value is minimized.

Keywords: Bypass surgery, Coronary artery stenosis, Distance from stenosis location, Graft angle.

1 | Introduction

Cardiovascular Diseases (CVDs) remain the leading cause of death globally, accounting for approximately 17.9 million deaths annually according to the World Health Organization. Among all CVDs, Coronary Artery Disease (CAD) is particularly prevalent, characterized by the buildup of atherosclerotic plaques within the coronary arteries, leading to stenosis or complete occlusion [1], [2]. This condition restricts blood flow to the myocardium, resulting in angina, myocardial infarction, and heart failure. Treatment options for CAD include pharmacotherapy, Percutaneous Coronary Intervention (PCI), and Coronary Artery Bypass Grafting (CABG) [3], [4].

 Corresponding Author: moradiankhadije@gmail.com

 <https://doi.org/10.48313/mtei.v2i3.61>



Licensee System Analytics. This article is an open access article distributed under the terms and conditions of the Creative Commons Attribution (CC BY) license (<http://creativecommons.org/licenses/by/4.0>).

CABG is considered the gold standard for patients with multivessel or left main CAD. In this surgical procedure, a healthy vessel (autograft) harvested from the leg (saphenous vein), chest (internal thoracic artery), or arm (radial artery) is anastomosed to create an alternative pathway upstream and downstream of the stenotic region [5]. Despite its clinical success, long-term patency of bypass grafts remains a major concern, with up to 50% of saphenous vein grafts failing within 10 years due to intimal hyperplasia and accelerated atherosclerosis.

Hemodynamic factors, particularly Wall Shear Stress (WSS), play a crucial role in graft failure. WSS is the frictional force exerted by flowing blood on the endothelial lining of the vessel wall. Low WSS (≤ 0.4 Pa) promotes endothelial dysfunction, inflammation, and intimal hyperplasia, while high WSS (≥ 4 Pa) can cause endothelial damage and platelet activation [6], [7]. Oscillatory shear stress, characterized by a high Oscillatory Shear Index (OSI), is also associated with atherogenic phenotypes [8], [9].

Geometric parameters of the bypass graft, including anastomotic angle and distance from the stenosis, significantly influence local hemodynamics. The graft angle affects flow separation, vortex formation, and WSS distribution at the toe and heel of the anastomosis. Numerous Computational Fluid Dynamics (CFD) studies have investigated optimal graft angles. For example, Recent advances in patient-specific modeling have further enhanced the clinical relevance of CFD simulations [10]. Several studies have successfully employed CFD to optimize bypass graft configurations [11].

Ogiso et al. [12] applied CFD to assess portal vein stenosis after liver transplantation, demonstrating that WSS analysis can predict and manage postoperative complications. Heidarinejad et al. [13] numerically investigated hemodynamic parameters of Y-bypass grafts under rest and exercise conditions, revealing significant WSS variations with flow rate.

Despite these contributions, most previous studies have examined either graft angle or distance separately, without considering their simultaneous effects. Moreover, few studies have focused on severe (95%) coronary stenosis, which represents a critical clinical scenario requiring urgent revascularization. Therefore, this article aims to simultaneously investigate the effects of graft angle (5° – 15°) and distance from stenosis (1–10 mm) on velocity and WSS in a 95% stenosed coronary artery model. Both steady and pulsatile flow conditions are examined to provide comprehensive guidance for optimal graft positioning in aortocoronary bypass surgery.

2 | Materials and Methods

In this research, blood flow is simulated using the Navier-Stokes equations in ANSYS Fluent software [14]. Velocity and WSS variations are investigated. Density and viscosity are 1.06 g/cm^3 and $0.004 \text{ Pa}\cdot\text{s}$, respectively [15]. The Finite Volume Method (FVM) solves the continuity and Navier-Stokes equations. Graft and host arteries are circular conduits with a 2 mm diameter. Blood flow moves within a bifurcation with a 5–15 degree angle. Vessel geometry is a cylindrical tube with a circular cross-section. All walls are rigid with a no-slip condition. Inlet velocity is constant and time-independent.

Table 1. Range of parameter variations.

Parameter	Symbol	Range	Unit
Graft angle	α	5–15	Degree
Distance from stenosis	X	1–10	mm
Stenosis percentage	R	95	%

3 | Governing Equations

Blood is a non-Newtonian fluid due to blood cells and plasma [1]. Shear stress results from forces parallel to the vessel wall [2]. Red blood cell shape and number affect shear stress [3]. Mass transfer at the vessel wall is strongly influenced by mechanical shear [4]. Shear stress is obtained from:

$$\tau = \mu \frac{du}{dz}, \quad (1)$$

where $\frac{du}{dz}$ is the velocity gradient perpendicular to the flow, and μ is viscosity [5]. WSS is defined as:

$$\text{WSS: } \vec{\tau}_w = \mu \frac{dw}{dl}, \quad (2)$$

where l is the distance to the wall, w is the velocity vector parallel to the wall [6]. The OSI quantifies the oscillatory nature of WSS [7]:

$$\text{OSI} = \frac{1}{2} \left(1.0 - \frac{\left| \int_0^T \vec{\tau}_w dt \right|}{\left| \int_0^T \vec{\tau}_w dt \right|} \right), \quad (3)$$

OSI ranges from 0 (no oscillation) to 0.5 (completely unstable) [7]. To solve the Navier-Stokes equations, appropriate boundary conditions must be specified:

- I. Inlet boundary condition (velocity inlet)
- II. Outlet boundary condition (pressure outlet)
- III. Wall boundary condition (no-slip condition): This condition is valid because blood is viscous and adheres to the vessel wall.
- IV. Symmetry (if applicable): In some simplified models, symmetry planes can be used to reduce computational cost

3.6 | Numerical Solution Method (Computational Fluid Dynamics Setup)

The governing equations are solved using the FVM in ANSYS Fluent 2023 R1 software. FVM discretizes the computational domain into a finite number of control volumes (cells) and converts the partial differential equations into algebraic equations that can be solved iteratively.

4 | Results and Discussion

Based on equations in Section 3 and simulation in Fluent, velocity and shear stress variations are investigated. The wall satisfies no-slip, and flow is three-dimensional, time-independent, incompressible, Newtonian, and homogeneous [8]. *Fig. 1* shows a schematic of the geometry.

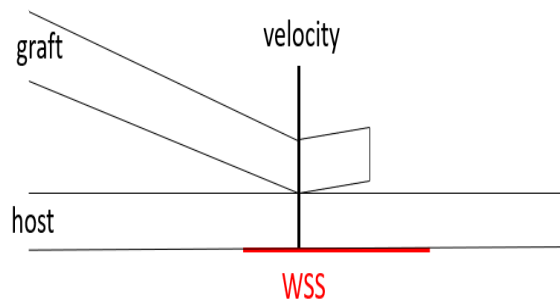


Fig. 1. Schematic of the geometry under investigation.

Fig. 2 shows the velocity contours for 95% stenosis at distances of 1, 5, and 10 mm from the stenosis and graft angles of 5°, 10°, and 15°. The maximum velocity occurs at the center of the stenosis, decreasing toward the walls due to the no-slip condition. At the anastomosis, a vortex forms due to flow impingement from the graft and host artery, creating a localized high-velocity region. When the anastomosis is placed at $X = 1$ mm, the stenotic jet reaches the junction before dissipating, producing a larger and more intense vortex. At $X =$

10 mm, the jet has expanded, resulting in a smaller vortex and lower peak velocity. Increasing the graft angle from 5° to 15° directs the flow more sharply against the opposite wall, enlarging the recirculation zone.

WSS; flow direction and geometry are equally important. The optimal configuration among the tested cases is X = 10 mm and α = 15°, which minimizes both velocity and WSS.

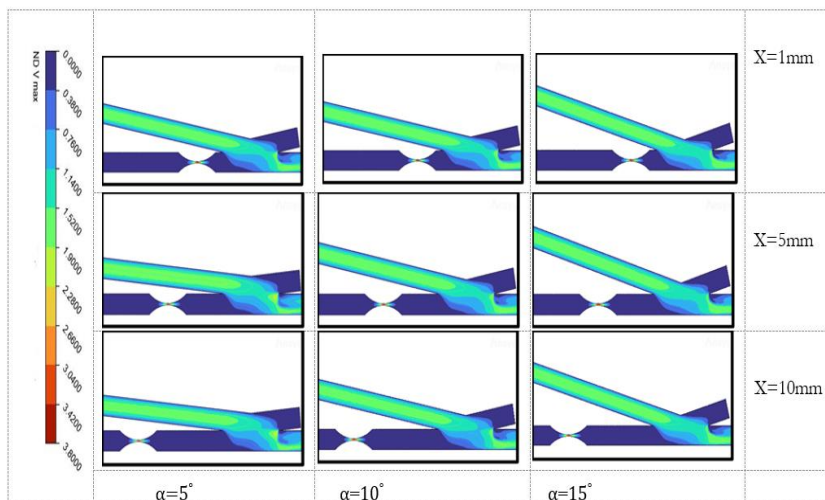
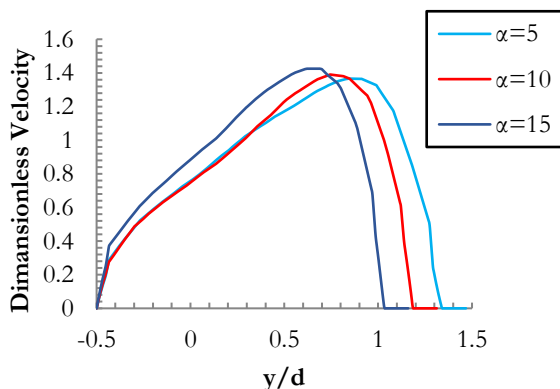


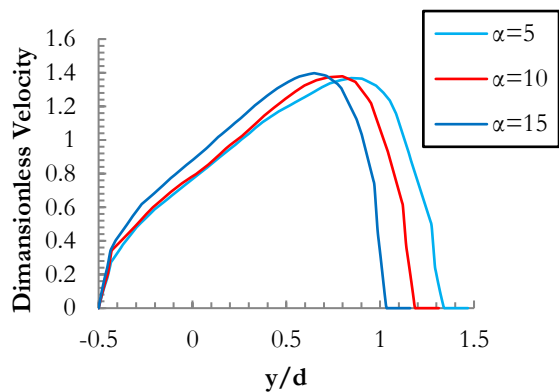
Fig. 2. Velocity contours at 95% stenosis.

Fig. 3 presents quantitative velocity variations along the coronary artery. The maximum recorded velocity is 1.4251 m/s at X = 1 mm and α = 15°, while the minimum is 1.33 m/s at X = 10 mm and α = 5°. Across all distances, the highest velocity occurs at α = 15° and the lowest at α = 5°, because a larger angle provides a more direct flow path. At X = 1 mm, the stenotic jet reaches the junction at full intensity. At X = 5 mm, partial expansion occurs, and a recirculation zone appears at the heel of the anastomosis. At X = 10 mm, the jet is fully expanded, yielding the most uniform velocity profile. The steepest velocity gradients occur at the toe of the anastomosis, directly correlating with WSS.

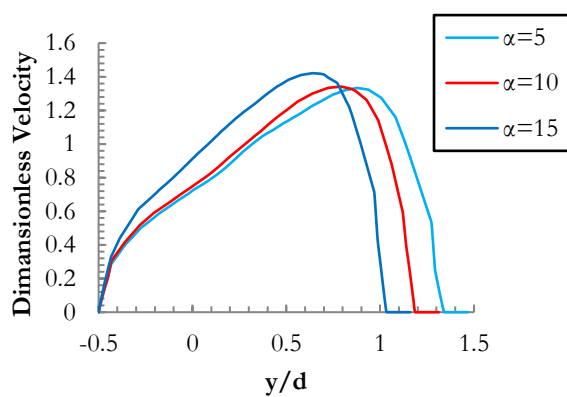
Fig. 4 depicts WSS distribution along the vessel wall. The maximum WSS is 40.72 Pa at X = 1 mm and α = 5°, while the minimum is 29.39 Pa at X = 10 mm and α = 15°, representing a 27.8% reduction. At X = 1 mm, WSS is dangerously high regardless of angle. At X = 5 mm, the highest WSS occurs at α = 5° due to direct flow impingement. At X = 10 mm, WSS is minimized at α = 15°, indicating that a larger angle combined with greater distance provides the most protective hemodynamic profile. Velocity magnitude alone does not determine.



a.

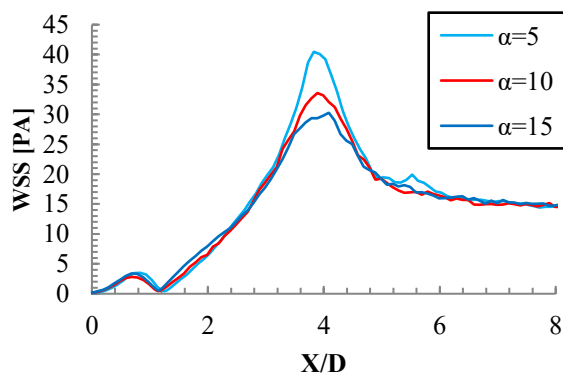


b.



c.

Fig. 3. Velocity variations at 95% stenosis at distances; a. 1 mm, b. 5 mm, c. 10 mm.



a.

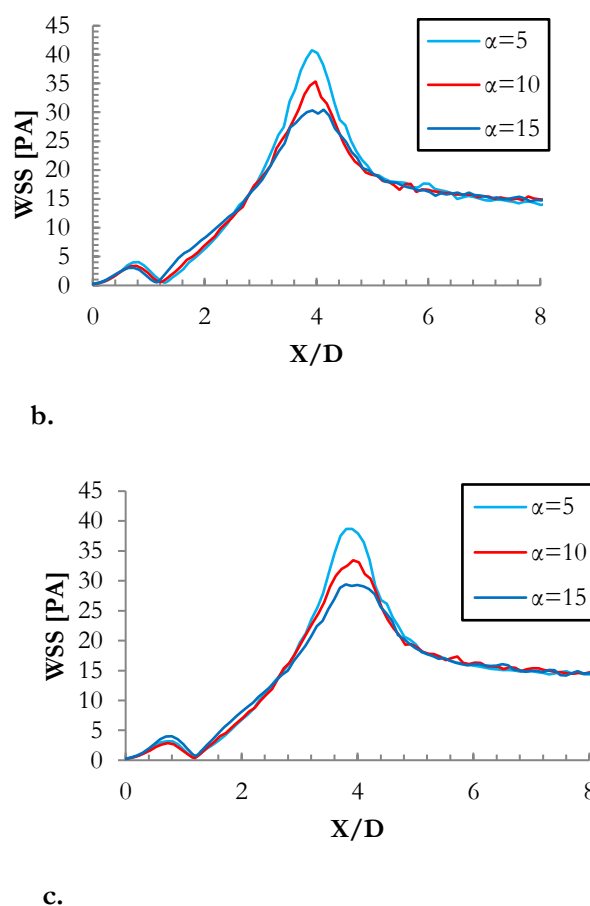


Fig. 4. Shear stress variations at 95% stenosis at distances; a. 1 mm, b. 5 mm, c. 10 mm.

5 | Conclusion

In this study, the impact of anastomotic angle (5° – 15°) and distance from stenosis (1–10 mm) on velocity and WSS in a 95% stenosed coronary artery bypass model using CFD was investigated. The results indicate that both parameters have a significant impact on hemodynamics. The maximum velocity (1.4251 m/s) was found at $X = 1$ mm and $\alpha = 15^\circ$, and the minimum (1.33 m/s) at $X = 10$ mm and $\alpha = 5^\circ$. The maximum WSS (40.72 Pa) at $X = 1$ mm and $\alpha = 5^\circ$ was well above the physiological value. The minimum WSS (29.39 Pa) at $X = 10$ mm and $\alpha = 15^\circ$ was 27.8% lower than the maximum. Placing the anastomosis too close to the stenosis is unfavorable for both angles. A too small angle (5°) at an intermediate distance (5 mm) creates a very dangerous impingement zone. The best situation is $X = 10$ mm and $\alpha = 15^\circ$, which minimizes both velocity and WSS. Increasing the distance from the stenosis is more effective in reducing the WSS than increasing the angle alone. From a clinical point of view, surgeons should consider placing the distal anastomosis at least 10 mm downstream of a severe stenosis and preferably with an angle of 15° , in order to maximize the long-term patency.

Conflict of Interest

The authors declare that there are no conflicts of interest regarding the publication of this paper.

Data Availability

The datasets generated and/or analyzed during the current study are included in this article.

Funding

This study was carried out without any specific funding from public, commercial, or non-profit organizations.

References

- [1] Libby, P. (2021). The changing landscape of atherosclerosis. *Nature*, 592(7855), 524–533. <https://doi.org/10.1038/s41586-021-03392-8>
- [2] Tsao, C. W., Aday, A. W., Almarzooq, Z. I., Anderson, C. A. M., Arora, P., Avery, C. L., ... & Martin, S. S. (2023). Heart disease and stroke statistics-2023 update: A report from the American Heart Association. *Circulation*, 147(8), e93–e621. <https://doi.org/10.1161/CIR.0000000000001123>
- [3] Neumann, F. J., Sousa-Uva, M., Ahlsson, A., Alfonso, F., Banning, A. P., Benedetto, U. (2019). 2018 ESC/EACTS guidelines on myocardial revascularization. *European Heart Journal*, 40(2), 87–165. <https://doi.org/10.1093/eurheartj/ehy394>
- [4] Serruys, P. W., Morice, M. C., Kappetein, A. P., Colombo, A., Holmes, D. R., Mack, M. J. (2009). Percutaneous coronary intervention versus coronary-artery bypass grafting for severe coronary artery disease. *New England journal of medicine*, 360(10), 961–972. <https://doi.org/10.1056/NEJMoa0804626>
- [5] Goldman, S., Zadina, K., Moritz, T., Ovitt, T., Sethi, G., Copeland, J. G (2004). Long-term patency of saphenous vein and left internal mammary artery grafts after coronary artery bypass surgery. *JACC*, 44(11), 2149–2156. <https://doi.org/10.1016/j.jacc.2004.08.064>
- [6] Malek, A. M., Alper, S. L., & Izumo, S. (1999). Hemodynamic shear stress and its role in atherosclerosis. *Jama*, 282(21), 2035–2042. <https://doi.org/10.1001/jama.282.21.2035>
- [7] Cunningham, K. S., & Gotlieb, A. I. (2005). Erratum: The role of shear stress in the pathogenesis of atherosclerosis. *Laboratory investigation*, 85(7), 942. <https://doi.org/10.1038/labinvest.3700215>
- [8] Ku, D. N. (1997). Blood flow in arteries. *Annual review of fluid mechanics*, 29(1), 399–434. <https://doi.org/10.1146/annurev.fluid.29.1.399>
- [9] Rassoli, A., Changizi, S., Soltani, F., & Gu, L. (2025). Understanding coronary bypass grafts from mechanical constitutive models to machine learning: A review. *Proceedings of the institution of mechanical engineers, part h: Journal of engineering in medicine*, 239(9), 857–871. <https://doi.org/10.1177/09544119251355753>
- [10] Eshtehardi, P., Brown, A. J., Bhargava, A., Costopoulos, C., Hung, O. Y., Corban, M. T., ... & Samady, H. (2017). High wall shear stress and high-risk plaque: An emerging concept. *The international journal of cardiovascular imaging*, 33(7), 1089–1099. <https://doi.org/10.1007/s10554-016-1055-1>
- [11] Liu, X., Sun, A., Fan, Y., & Deng, X. (2015). Physiological significance of helical flow in the arterial system and its potential clinical applications. *Annals of biomedical engineering*, 43(1), 3–15. <https://doi.org/10.1007/s10439-014-1097-2>
- [12] Ogiso, S., Nakamura, M., Tanaka, T., Komiya, K., Kamei, H., Onishi, Y., ... & Ogura, Y. (2020). Computational fluid dynamics-based blood flow assessment facilitates optimal management of portal vein stenosis after liver transplantation. *Journal of gastrointestinal surgery*, 24(2), 460–461. <https://doi.org/10.1007/s11605-019-04279-w>
- [13] Heidarinejad, G., Babakhani, H., & Rostami, A. (2020). Numerical study of the hemodynamic parameters of the Y-bypass graft at rest and exercise state. *Amirkabir journal of mechanical engineering*, 51(6), 1325–1338. https://mej.aut.ac.ir/jufile?ar_sfile=79705
- [14] Fluent, A. (2023). *Ansys Fluent Theory Guide*. <https://cir.nii.ac.jp/crid/1370588380133657489>
- [15] Reza Haghighi, A., & Shahbazi Asl, M. (2015). Numerical simulation of unsteady blood flow through an elastic artery with a non-symmetric stenosis. *Modares mechanical engineering*, 14(10), 26-34. **(In Persian)**. https://journals.modares.ac.ir/article_8164_a70145bf8b173e4496b554ce57969e24.pdf